JACS ARTICLES
Published on Web 08/25/2004

Bulk versus Interfacial Aqueous Solvation of Dicarboxylate Dianions

Babak Minofar,[†] Martin Mucha,[†] Pavel Jungwirth,*,[†] Xin Yang,[‡] You-Jun Fu,[‡] Xue-Bin Wang,[‡] and Lai-Sheng Wang*,[‡]

Contribution from the Institute of Organic Chemistry and Biochemistry, Academy of Sciences of the Czech Republic and Center for Complex Molecular Systems and Biomolecules, Flemingovo nam. 2, 16610 Prague 6, Czech Republic, Department of Physics, Washington State University, 2710 University Drive, Richland, Washington 99352, and W. R. Wiley Environmental Molecular Sciences Laboratory, Pacific Northwest National Laboratory, P.O. Box 999, Richland, Washington 99352

Received April 29, 2004; E-mail: pavel.jungwirth@uochb.cas.cz; ls.wang@pnl.gov

Abstract: Solvation of dicarboxylate dianions of varying length of the aliphatic chain in water clusters and in extended aqueous slabs was investigated using photoelectron spectroscopy and molecular dynamics simulations. Photoelectron spectra of hydrated succinate, adipate, and tetradecandioic dianions with up to 20 water molecules were obtained. Even−odd effects were observed as a result of the alternate solvation mode of the two negative charges with increasing solvent numbers. The competition between hydrophilic interactions of the charged carboxylate groups and hydrophobic interactions of the aliphatic chain leads to conformation changes in large water clusters containing dicarboxylates bigger than adipate. It also leads to a transition from bulk aqueous solvation of small dicarboxylates to solvation at the water/vapor interface of the larger ones. Whereas oxalate and adipate solvate in the inner parts of the aqueous slab, suberate and longer dicarboxylate dianions have a strong propensity to the surface. This transition also has consequences for the folding of the flexible aliphatic chain and for the structure of aqueous solvation shells around the dianions.

1. Introduction

The propensity of certain atomic and small molecular ions for the water/vapor interface has important implications for heterogeneous chemistry at aqueous surfaces. In particular, important tropospheric reactions involving polluting gases such as ozone or OH and leading to the production of reactive halogen compounds take place at the surface of aqueous sea salt aerosols in the lower marine troposphere[1,2] or salt solution films sprayed over the polar snowpack.[3] There is mounting computational and experimental evidence that heavier halides (iodide, bromide, and, to a lesser extent, chloride) penetrate the aqueous surface, where they can react with atmospheric gases.[4] Among small molecular ions, nitrate and azide were also shown to exhibit a similar surface behavior.[5,6] Note that the propensity for the water/vapor interface of these ions cannot be attributed to hydrophobicity since they lack any hydrophobic center. Results of molecular dynamics (MD) simulations indicate that in these cases the main force that drives the above anions to the aqueous surface is their large polarizability (softness).[4,7,8]

Small *multiply* charged ions exhibit a more pronounced hydrophilicity than those bearing a single elementary charge. Because of the strong electrostatic interactions with surrounding water molecules, they tend to organize in the bulk liquid one to two solvation shells around themselves. These ions are repelled from the water/vapor interface because of huge image forces. As a result, they never penetrate into the topmost surface layer of aqueous systems. Typical examples of positively charged ions are alkali earth dications such as Mg^{2+} or Ca^{2+}, while SO_4^{2-} represents a textbook hydrophilic dianion.[9]

Gas-phase solvated clusters provide ideal molecular models for investigating the solvation behaviors of atomic and molecular ions and can provide valuable information pertaining to the question of bulk vs interfacial solvation.[10−15] For the heavier

[†] Academy of Sciences of the Czech Republic and Center for Complex Molecular Systems and Biomolecules.

[‡] Washington State University and Pacific Northwest National Laboratory.

(1) Oum, K. W.; Lakin, M. J.; DeHaan, D. O.; Brauers, T.; Finlayson-Pitts, B. J. *Science* **1998**, *279*, 74−77.
(2) Knipping, E. M.; Lakin, M. J.; Foster, K. L.; Jungwirth, P.; Tobias, D. J.; Gerber, R. B.; Dabdub, D.; Finlayson-Pitts, B. J. *Science* **2000**, *288*, 301−306.
(3) Foster, K. L.; Plastridge, R. A.; Bottenheim, J. W.; Shepson, P. B.; Finlayson-Pitts, B. J.; Spicer, C. W. *Science* **2001**, *291*, 471−474.
(4) Jungwirth, P.; Tobias, D. J. *J. Phys. Chem. B* **2002**, *106*, 6361−6373.
(5) Salvador, P.; Curtis, J. E.; Tobias, D. J.; Jungwirth, P. *Phys. Chem. Chem. Phys.* **2003**, *5*, 3752−3757.
(6) Yang, X.; Kiran, B.; Wang, X. B.; Wang, L. S.; Mucha, M.; Jungwirth, P. *J. Phys. Chem. A*, published online May 8, 2004, http://dx.doi.org/10.1021/jp0496396.
(7) Jungwirth, P.; Tobias, D. J. *J. Phys. Chem. B* **2001**, *105*, 10468−10472.
(8) Dang, L. X.; Chang, T. M. *J. Phys. Chem. B* **2002**, *106*, 235−238.
(9) Jungwirth, P.; Curtis, J. E.; Tobias, D. J. *Chem. Phys. Lett.* **2003**, *367*, 704−710.
(10) Greenblatt, B. J.; Zanni, M. T.; Neumark, D. M. *Science* **1997**, *276*, 1675−1678.
(11) Cabarcos, O. M.; Weinheimer, C. J.; Lisy, J. M.; Xantheas, S. S. *J. Chem. Phys.* **1999**, *110*, 5−8.

halogen ions (Cl^-, Br^-, and I^-) and azide (N_3^-), which have a propensity for the water/vapor interface of extended systems, studies of their hydrated clusters demonstrate that they also prefer a "surface" solvation state.[6,16−21] An interesting class of systems are multiply charged ions.[22−26] Recent experimental advances using photoelectron spectroscopy and electrospray have allowed multiply charged anions to be studied in the gas phase.[27,28] Hydrated clusters of small multiply charged anions including SO_4^{2-} have been produced and shown that these species prefer to be in the center of the solvated clusters,[29−31] anticipating their absence from the air/water interface in extended systems or nanodroplets.[9]

In contrast to the above small multiply charged ions, dicarboxylate dianions $^-O_2C-(CH_2)_n-CO_2^-$ have two distinct charged groups ($-CO_2^-$) linked by a flexible hydrophobic aliphatic chain. Recently, we have investigated the sequential solvation of an example of dicarboxylate dianions, $^-O_2C-(CH_2)_6-CO_2^-$ (suberate), in clusters with 1−25 water molecules in a combined photoelectron spectroscopy and computational study.[32] The main finding is that for up to about 16 water molecules, both carboxylate charge centers of the linear gas phase dianion are separately solvated, one water molecule after another in an alternating pattern. However, upon adding more waters, the suberate dianion folds and a single water cluster forms around and between the two $-CO_2^-$ groups. At the same time, the hydrophobic $(CH_2)_6$ chain is not solvated by water molecules at all, regardless of the cluster size.

Dicarboxylate dianions play important roles in many natural environments. For example, carboxylate is an important negative charge carrier in proteins, which is present in the C-terminal of polypeptides and the side chains of aspartic and glutamic acids. As another example, dicarboxylate dianions originating from small, water soluble acids (such as oxalic, malonic, or succinic acid) were recently suggested to play an important role in controlling the chemical and physical properties of organic aerosols in the polluted troposphere.[33] Understanding the solvation behavior in aqueous interfaces of the dicarboxylate dianions may be essential to elucidate the chemistry of the organic aerosols containing these species.

These dianions with a varying length of the $(CH_2)_n$ chain also represent ideal systems for studying the competition between hydrophilic electrostatic forces due to the $-CO_2^-$ groups and the hydrophobic interactions between the connecting aliphatic chain and water.[34,35] In the current work, we report a comprehensive experimental and theoretical study on a series of dicarboxylate dianions with different numbers of CH_2 spacer groups. Experimentally, we have obtained photoelectron spectra for hydrated $^-O_2C-(CH_2)_n-CO_2^-$ for $n = 2$, 4, 12, and up to 20 water molecules. There are two questions that we would like to address. Previous work has shown that the smallest member of the series, the oxalate ($C_2O_4^{2-}$), prefers to be in the center of the solvated clusters.[30,31] As the aliphatic chain length is increased, the size of the dianion increases and the hydrophobic interactions with water also increase. What is the largest dicarboxylate that can still have the interior solvation behavior? Second, we want to examine how the solvation-induced conformation change would depend on the aliphatic chain length, as well as on the number of solvent molecules.

Despite the above cluster results, there is little direct information about the character of solvation of dicarboxylate dianions in extended aqueous systems. While, as discussed above, a lot of valuable information is gained from cluster studies, solvation at the extended water/vapor interface differs somewhat from that in and on aqueous clusters with a diameter smaller than about 100 nm because of the finite size and surface curvature of the latter. In particular, the curved surface of the aqueous cluster represents a possible additional surface driving factor for the solute species, which is missing at the planar interface of extended systems.[36] Extensive molecular dynamics simulations have thus been carried out within the current study concerning the solvation and, in particular, the interfacial behaviors of the dicarboxylates with different aliphatic chain lengths. The main questions addressed, in conjunction with the experimental work, which focused on small- and medium-sized solvated clusters, are as follows: Do small dicarboxylate dianions solvate in the aqueous bulk, and do the larger ones solvate at the water/vapor interface? At what length of the aliphatic chain do the hydrophobic interactions overwhelm the hydrophilic ones, leading to a crossover between bulk and surface solvation? To what extent is the dicarboxylate dianion folded and unfolded at the surface and in the aqueous bulk? What is the solvent structure around the charged carboxylate groups and around the aliphatic chain? In addition, the experiment addresses the issues of sequential hydration and possible folding of dicarboxylate dianions upon increasing the number of solvent water molecules, as observed recently for suberate.[32]

In our previous work on clusters containing a suberate dianion and up to 20 water molecules,[32] quantitative agreement between computer simulations and results of photoelectron spectroscopy measurements was established. Building on this success, in the present study we employ experiment and computations primarily in a complementary way, the former focusing on extracting

(12) Ayotte, P.; Weddle, G. H.; Johnson, M. A. *J. Chem. Phys.* **1999**, *110*, 7129−7132.
(13) Lehr, L.; Zanni, M. T.; Frischkorn, C.; Weinkauf, R.; Neumark, D. M. *Science* **1999**, *284*, 635−638.
(14) Weber, J. M.; Kelley, J. A.; Nielsen, S. B.; Ayotte, P.; Johnson, M. A. *Science* **2000**, *287*, 2461−2463.
(15) Patwari, G. N.; Lisy, J. M. *J. Chem. Phys.* **2003**, *118*, 8555−8558.
(16) Perera, L.; Berkowitz, M. L. *J. Chem. Phys.* **1991**, *95*, 1954−1963.
(17) Perera, L.; Berkowitz, M. L. *J. Chem. Phys.* **1992**, *96*, 8288−8294.
(18) Perera, L.; Berkowitz, M. L. *J. Chem. Phys.* **1993**, *99*, 4222−4224.
(19) Stuart, S. J.; Berne, B. J. *J. Phys. Chem.* **1996**, *100*, 11934−11943.
(20) Markovich, G.; Pollack, S.; Giniger, R.; Cheshnovsky, O. *J. Chem. Phys.* **1994**, *101*, 9344−9353.
(21) Choi, J. H.; Kuwata, K. T.; Cao, Y. B.; Okumura, M. *J. Phys. Chem. A* **1998**, *102*, 503−507.
(22) Kalcher, J.; Sax, A. F. *Chem. Rev.* **1994**, *94*, 2291−2318.
(23) Freeman, G. R.; March, N. H. *J. Phys. Chem.* **1996**, *100*, 4331−4338.
(24) Boldyrev, A. I.; Gutowski, M.; Simons, J. *Acc. Chem. Res.* **1996**, *29*, 497−502.
(25) Stefanovich, E. V.; Boldyrev, A. I.; Truong, T. N.; Simons, J. *J. Phys. Chem. B* **1998**, *102*, 4205−4208.
(26) Dreuw, A.; Cederbaum, L. S. *Chem. Rev.* **2002**, *102*, 181−200.
(27) Wang, L. S.; Wang, X. B. *J. Phys. Chem. A* **2000**, *104*, 1978−1990.
(28) Wang, X. B.; Yang, X.; Wang, L. S. *Int. Rev. Phys. Chem.* **2002**, *21*, 473−498.
(29) Yang, X.; Wang, X. B.; Wang, L. S. *J. Phys. Chem. A* **2002**, *106*, 7607−7616.
(30) Wang, X. B.; Yang, X.; Nicholas, J. B.; Wang, L. S. *J. Chem. Phys.* **2003**, *119*, 3631−3640.
(31) Wang, X. B.; Yang, X.; Nicholas, J. B.; Wang, L. S. *Science* **2001**, *294*, 1322−1325.
(32) Yang, X.; Fu, Y. J.; Wang, X. B.; Slavicek, P.; Mucha, M.; Jungwirth, P.; Wang, L. S. *J. Am. Chem. Soc.* **2004**, *126*, 876−883.
(33) Kawamura, K.; Umemoto, N.; Mochida, M.; Bertram, T.; Howell, S.; Huebert, B. J. *J. Geophys. Res., D: Atmos.* **2003**, *108* 8639.
(34) Wang, L. S.; Ding, C. F.; Wang, X. B.; Nicholas, J. B. *Phys. Rev. Lett.* **1998**, *81*, 2667−2670.
(35) Ding, C. F.; Wang, X. B.; Wang, L. S. *J. Phys. Chem. A* **1998**, *102*, 8633−8636.
(36) Stuart, S. J.; Berne, B. J. *J. Phys. Chem. A* **1999**, *103*, 10300−10307.

electron binding energies and inferring structures of dicarboxylate dianions in and on water clusters, while the latter aiming at elucidating directly the thermodynamically averaged structures of these dianions in the aqueous bulk or at the extended water/vapor interface.

2. Experimental and Computational Methods

2.1. Photoelectron Spectroscopy. The experiment was carried out using an apparatus equipped with a magnetic-bottle time-of-flight photoelectron analyzer and an ESI source.[37] Details of the experimental method have been given elsewhere,[37] and the procedures were the same as our previous study on the solvated suberate dianions.[32] Briefly, solvated dianions with a wide range of solvent molecules, $^{-}O_2C(CH_2)_n$-$CO_2^{-}(H_2O)_x$, were produced from electrospray of mixed solutions of 10^{-3} M of the corresponding acids, $HO_2C(CH_2)_nCO_2H$ and 2×10^{-3} M NaOH in a water−acetonitrile mixture (1:4 volume ratio). Anions produced from the ESI source were guided into a room-temperature ion trap, where ions were accumulated for 0.1 s before being pulsed into the extraction zone of a time-of-flight mass spectrometer. During photoelectron spectroscopic experiments, the dianions of interest were mass-selected and decelerated before being intercepted by a probe laser beam in the photodetachment zone of the magnetic-bottle photoelectron analyzer. In the current study, the detachment photon energy was 193 nm (6.424 eV). Photoelectron time-of-flight spectra were collected and then converted to kinetic energy spectra, calibrated by the known spectra of I^- and O^-. The electron binding energies (EB) were obtained by subtracting the kinetic energy (KE) spectra from the detachment photon energy (EB = 6.424 eV − KE). The energy resolution (ΔKE/KE) was about 2%, i.e., ~10 meV for 0.5 eV electrons, as measured from the spectrum of I^- at 355 nm.

2.2. Computational Methods. The calculations involved classical molecular dynamics simulations aimed at a Boltzmann sampling of solvation structures of $^{-}O_2C(CH_2)_nCO_2^{-}$, $n = 0$, 4, 6, and 12 (i.e., oxalate, adipate, suberate, and tetradecandioic dianion) in and on aqueous slabs. To construct the slab, a rectangular box of $3.5 \times 3.5 \times 17.5$ nm^3 was used, containing 1400 water molecules, a single dicarboxylate dianion, and two sodium cations as counterions. Application of periodic boundary conditions at constant volume with such a unit cell yields an infinite slab with two open surfaces, perpendicular to the z-axis. A cutoff of 16 Å was used for nonbonded interactions. Long-range electrostatic interactions were accounted for using a standard particle mesh Ewald procedure.[38]

The systems were first equilibrated at 300 K for at least 0.5 ns, after which very long (~5 ns) production runs at the same temperature followed. A time step of 1 fs was adopted, and all bonds containing hydrogen atoms were constrained using the standard SHAKE procedure.[39] We employed the SPCE model of water,[40] while for the dicarboxylate dianions, we used the Cornell force field[41] with fractional charges evaluated (as is the standard for force field parametrizations[42]) at the HF/6-31G* level using the natural population analysis for structures optimized at the MP2/6-31$^+$G* level. All molecular dynamics calculations were performed using the GROMACS 3.1 program package.[43]

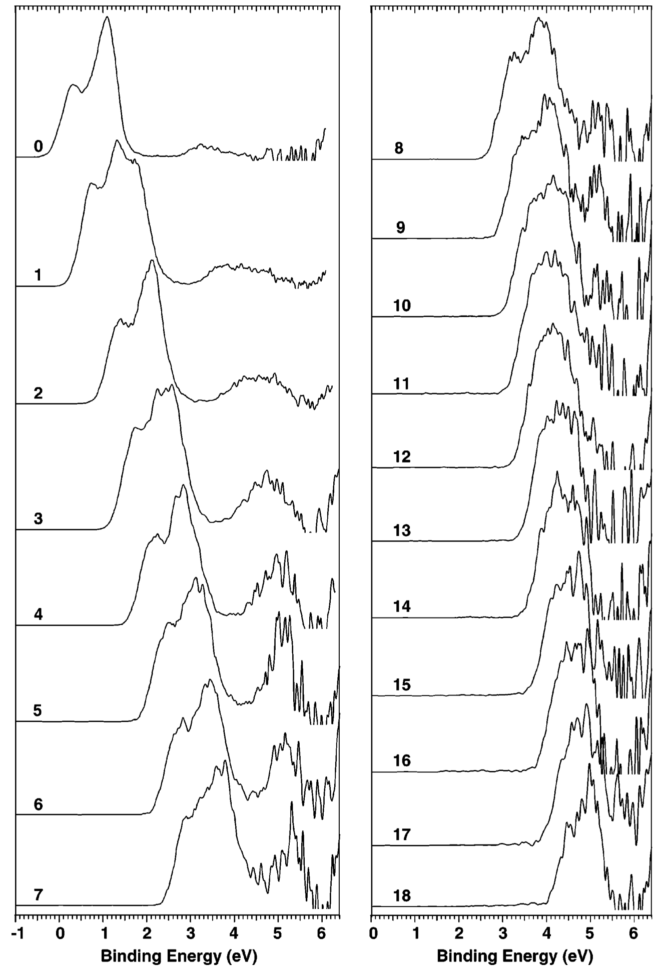

Figure 1. Photoelectron spectra of $^{-}O_2C-(CH_2)_2-CO_2^{-}(H_2O)_x$ ($x = 0-18$) at 193 nm (6.424 eV). Note the low electron binding energies of the bare anion at $x = 0$.

3. Experimental Results and Discussion

3.1. The Bare Dianions and the Observation of the Smallest Stable Dicarboxylate Dianions: The Succinate. The photoelectron spectra of $^{-}O_2C(CH_2)_nCO_2^{-}(H_2O)_x$ ($x = 0-20$) for $n = 2$, 4, 12 are displayed in Figures 1−3, respectively. The spectra of the bare dianions all exhibited two bands, consistent with our previous study carried out at two lower photon energies.[34] The weak band at higher binding energies in the spectra of the bare dianions was due to detachment of the singly charged anions by a second photon. The succinate dianion was observed for the first time here and was found to be barely stable with an adiabatic detachment energy (ADE) estimated as ~0.0 eV. We were not able to observe this dianion in our previous study,[44] likely because of a harsher desolvation condition in the electrospray source. The observed vanishing value of ADE for succinate qualitatively agrees with a previous ab initio calculation, which gives an ADE of −0.086 eV.[44] We have shown previously that the oxalate dianion ($C_2O_4^{2-}$) is not stable in the gas phase,[30,31] similarly to the sulfate dianion (SO_4^{2-}).[45,46] The succinate dianion turns out to be the smallest electronically stable dicarboxylate dianion in the gas phase, if

(37) Wang, L. S.; Ding, C. F.; Wang, X. B.; Barlow, S. E. *Rev. Sci. Instrum.* **1999**, *70*, 1957−1966.
(38) Essmann, U.; Perera, L.; Berkowitz, M. L.; Darden, T.; Lee, H.; Pedersen, L. G. *J. Chem. Phys.* **1995**, *103*, 8577−8593.
(39) Allen, M. P.; Tildesley, D. J. *Computer Simulations of Liquids*; Clarendon: Oxford, 1987.
(40) Berendsen, H. J. C.; Grigera, J. R.; Straatsma, T. P. *J. Phys. Chem.* **1987**, *91*, 6269−6271.
(41) Cornell, W. D.; Cieplak, P.; Bayly, C. I.; Gould, I. R.; Merz, K. M.; Ferguson, D. M.; Spellmeyer, D. C.; Fox, T.; Caldwell, J. W.; Kollman, P. A. *J. Am. Chem. Soc.* **1995**, *117*, 5179−5197.
(42) Bayly, C. I.; Cieplak, P.; Cornell, W. D.; Kollman, P. A. *J. Phys. Chem.* **1993**, *97*, 10269−10280.
(43) Lindahl, E.; Hess, B.; van der Spoel, D. *J. Mol. Model.* **2001**, *7*, 306−317.
(44) Skurski, P.; Simons, J.; Wang, X. B.; Wang, L. S. *J. Am. Chem. Soc.* **2000**, *122*, 4499−4507.
(45) Boldyrev, A. I.; Simons, J. *J. Phys. Chem.* **1994**, *98*, 2298−2300.
(46) Wang, X. B.; Nicholas, J. B.; Wang, L. S. *J. Chem. Phys.* **2000**, *113*, 10837−10840.

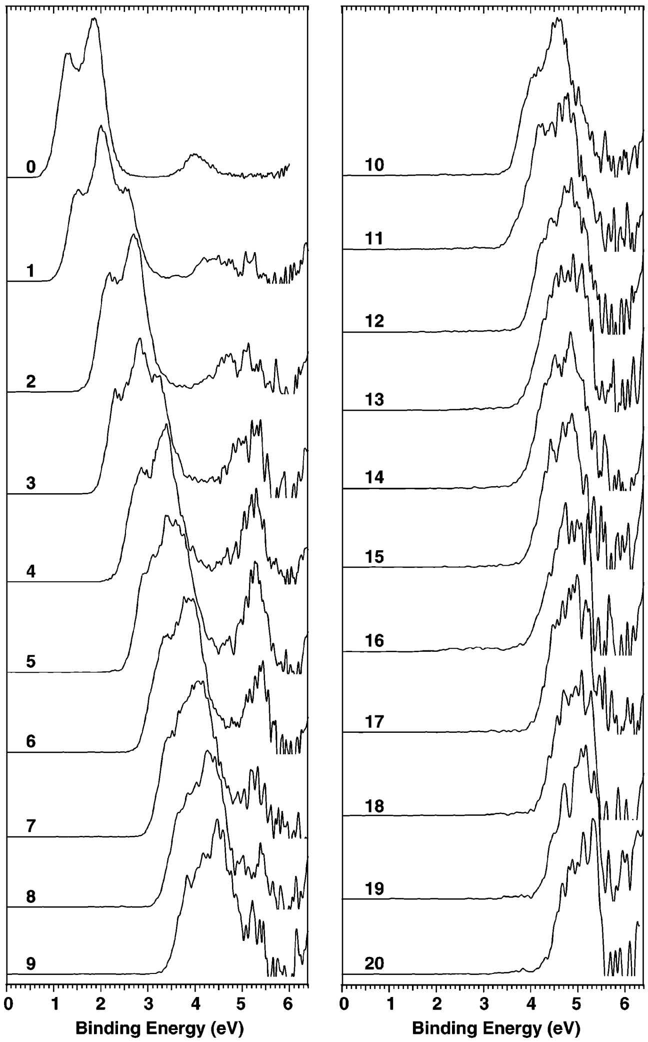

Figure 2. Photoelectron spectra of $^{-}O_2C-(CH_2)_4-CO_2^{-}(H_2O)_x$ ($x = 0-20$) at 193 nm.

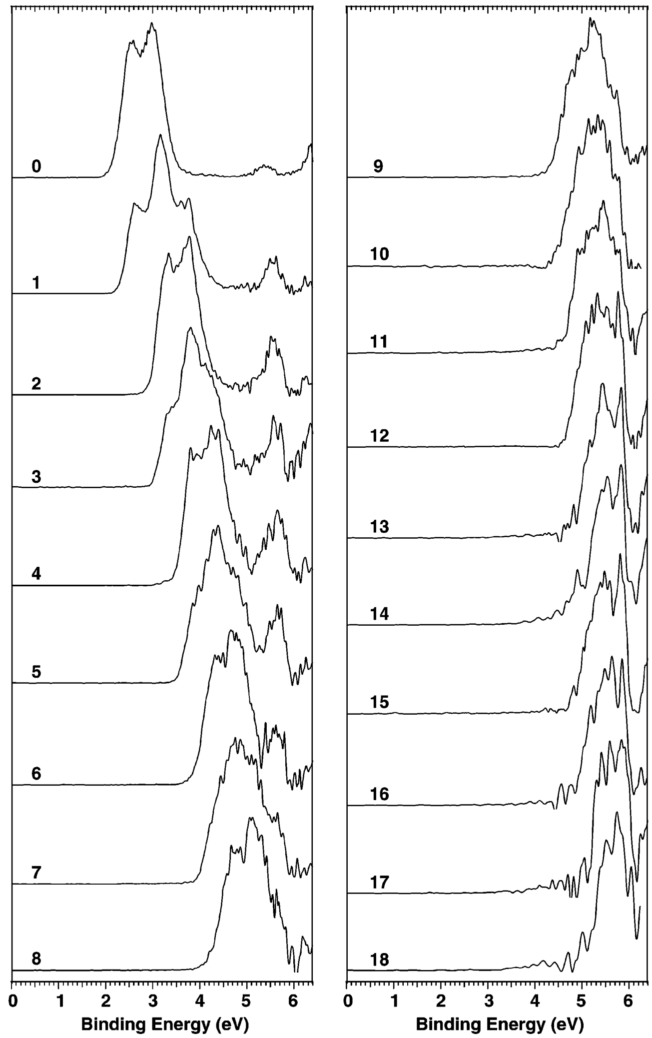

Figure 3. Photoelectron spectra of $^{-}O_2C-(CH_2)_{12}-CO_2^{-}(H_2O)_x$ ($x = 0-18$) at 193 nm.

only barely. The malonate dianion, which lies between oxalate and succinate in size, is expected to be unstable, and we have indeed failed to observe it in our electrospray source. In an unpublished work, we showed that we could readily observe malonate with three waters, $^{-}O_2CCH_2CO_2^{-}(H_2O)_3$, indicating that one to three water molecules are needed to stabilize the malonate dianion in the gas phase. We also showed previously that oxalate requires at least three waters to be stabilized.[30,31]

3.2. Hydrated Succinate, Adipate, and Tetradecandioic Dianions. The first solvent molecule caused the spectra of the dicarboxylate to split, as previously observed for the suberate system.[32] The first water can only solvate one of the $-CO_2^{-}$ groups, thus making the two carboxylate groups nonequivalent. The spectra of systems with two waters closely resemble those of the bare dianions, indicating that each water solvates one $-CO_2^{-}$ group separately. This even−odd pattern became difficult to recognize beyond four solvent waters for succinate and adipate, whereas for the hydrated suberate[32] and tetradecandioic dianions such even−odd changes were discernible for up to nine solvent molecules. The even−odd changes demonstrated that the water molecules tended to solvate the two $-CO_2^{-}$ groups independently and alternately. For large solvated dianions, the cluster intensity became relatively weak and the photoelectron spectral signal-to-noise ratios became poor. The high binding energy part of the spectra for the very large solvated clusters was cut off because of the repulsive Coulombic barrier universally present in multiply charged anions.[34] For $x = 1-7$, the weak feature at higher binding energies gained intensity and became broader. The binding energy of this feature seems to depend on the solvent number very weakly. We suspect that this weak band could also have contributions from ionization of the solvent, as was observed previously in the photoelectron spectra of hydrated sulfate and oxalate.[31]

3.3. Interior vs Exterior Solvation and Solvent-Induced Conformational Changes. The ADEs, estimated from the threshold of the photoelectron spectra shown in Figures 1−3, are plotted as a function of solvent number (x) in Figure 4a. The differential ADE (ΔADE), defined as [ADE($x + 1$) − ADE(x)], is the net stabilization of one water to the negative charge as water is sequentially added. It is plotted in Figure 4b as a function of x.

3.3.1. $^{-}O_2C(CH_2)_2CO_2^{-}(H_2O)_x$. The ADEs of the hydrated succinate exhibit a relatively smooth increase with the solvent number. The even−odd effect in the ADE is not very strong and seems to completely smooth out beyond five waters. These observations are consistent with the small size of succinate. Namely, after the first five or six waters, additional solvent can build around the dianion and effectively stabilize both negative

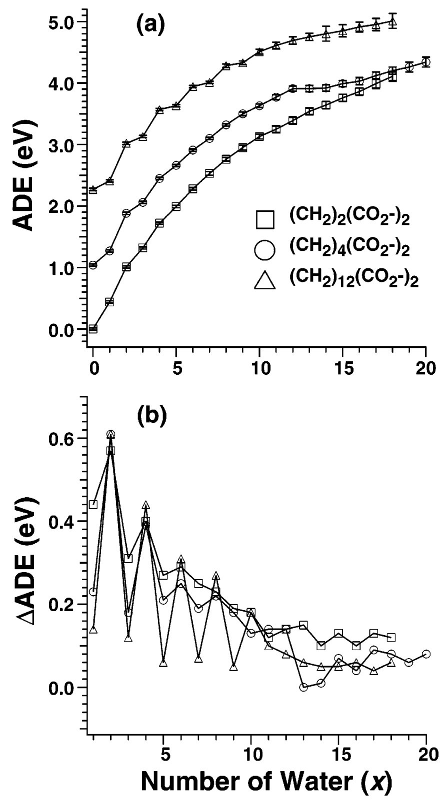

Figure 4. (a) Adiabatic electron binding energies (ADE) of hydrated succinate (□), adipate (○), and the tetradecandioic (△) dianions as a function of solvent numbers (x). (b) The differential ADE [$\Delta ADE = ADE(x + 1) - ADE(x)$] as a function of x.

charges more or less equally. This suggests an interior solvation state for succinate, analogous to sulfate and oxalate.[31] It is also expected that succinate prefers bulk solvation in extended aqueous systems.

3.3.2. $^-O_2C(CH_2)_4CO_2^-(H_2O)_x$. The ADE of the hydrated adipate as a function of the number of solvent molecules is more intriguing (Figure 4). First, the ΔADEs exhibited more pronounced even−odd changes than those of the succinate systems and tapered off beyond about eight waters. The ADEs then increased smoothly with x up to 12. But change in the slope was observed between $x = 12$ and 13: the ADEs of $x = 13$ and 14 showed no or little increase relative to that of $x = 12$. This is an indication of a conformation change. Previously, we observed that for the hydrated suberate systems folding takes place at $x = 16$, where the quasi-linear suberate dianion became bent and the two separately solvated $-CO_2^-$ centers merged.[32] The folding was caused by the strong cooperative H-bonding interactions between the solvent molecules and the hydrophobicity of the aliphatic chain. In the suberate systems, a dramatic ADE decrease was observed between the folded conformation at $x = 16$ relative to the unfolded conformation at $x = 15$. This is a result of the increased Coulombic repulsion upon folding, which brought the two negative charges closer to each other. Adipate has a shorter chain of four CH_2 spacer groups, which is not long enough to allow for such a dramatic folding structural change. But the ADE behavior between $x = 12$ and 13 signals a conformation change that brings the two carboxylates slightly closer to each other at $x = 13$. The fact that this happens at a smaller solvent number than in suberate is a manifestation of both the smaller size of adipate and the strong water−water interactions. At $x = 13$ and beyond, it is expected that the two separately solvated centers merge. Our current clusters were not large enough to extrapolate whether adipate assumes an interior or exterior solvation state in extended aqueous systems. Our computational study, described in detail below, suggests that adipate, as an intermediate size dicarboxylate dianion, prefers bulk solvation.

3.3.3. $^-O_2C(CH_2)_{12}CO_2^-(H_2O)_x$. The tetradecandioic dianion is the largest dicarboxylate systems that we have investigated. Its ADEs exhibit the most pronounced even−odd changes (Figure 4) since the two carboxylate groups are far apart and the solvation of each is almost independent of the other. However, the even−odd changes in the ADEs taper off beyond $x = 10$. This observation implies that five waters are needed to completely solvate the carboxylates on each end of the tetradecandioic dianion, presumably forming the first solvation shell. Additional waters exert a relatively small stabilization to the negative charges. Also, the even−odd effect was not measurable because of the large experimental uncertainty for large clusters, which were more difficult to produce because of the low solubility of this dianion. In analogy to the hydrated suberate systems, we expected that folding should happen for the tetradecandioic dianion at a certain solvation level. Because of the large distance between the two negative charge centers, a much more dramatic decrease in ADE was anticipated upon folding for the tetradecandioic dianion. It is apparent from the spectra that folding would require more solvent molecules than we were able to produce in our current experiment. The fact that the critical size is large (beyond those experimentally accessible) can be expected from the significant entropic contribution to the stability of the quasi-linear conformation at finite temperatures.[32] Twice as large as suberate, the tetradecandioic dianion is expected to prefer surface solvation with its hydrophobic aliphatic chains pointing into the vapor phase. This is exactly born out from the MD simulations presented below.

4. Computational Results and Discussion

4.1. Oxalate: $C_2O_4^{2-}$. The smallest dicarboxylate dianion, oxalate, does not contain any hydrophobic CH_2 groups. Experimentally, it was shown to sit in the center of water clusters, similarly to other small hydrophilic dianions (such as sulfate).[31] It was thus expected to solvate deeply in the aqueous bulk. This is indeed confirmed by the present MD simulations. Figure 5a shows the density profiles of the individual atomic species, i.e., histogrammed occurrences of the oxygen and carbon atoms of oxalate, the sodium counterions, and water oxygens across the water slab, averaged over the MD simulation. The water oxygen signal defines the extension of the slab, with an aqueous bulk region surrounded from both sides by a water/vapor interface. The signals from both oxalate oxygens and carbons clearly show that the smallest dicarboxylate dianion is strongly repelled from the aqueous surface and solvates deeply in the bulk region of the slab. As for aqueous sodium chloride, the sodium counterions are also, albeit somewhat less strongly, repelled from the water/vapor interface.

4.2. Adipate: $^-O_2C(CH_2)_4CO_2^-$. The next investigated aqueous dicarboxylate dianion − adipate, contains in addition to the two carboxylate groups a short aliphatic chain containing four CH_2 groups. The result of competition between the

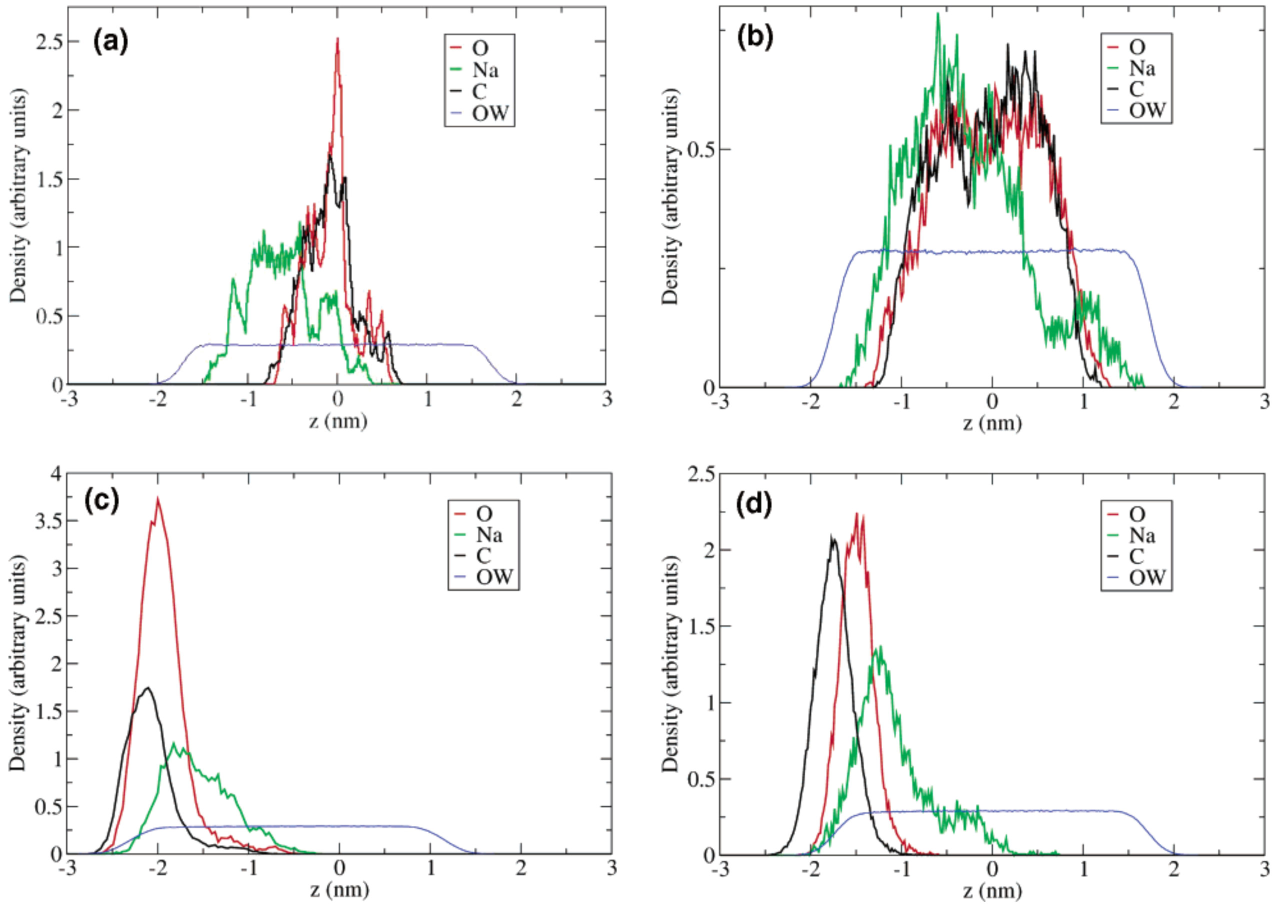

Figure 5. Density profiles of dicarboxylate dianions in an aqueous slab. Color coding: red, carboxylate oxygen; black, carbon; green, sodium counterions; and blue, water oxygen. (a) Oxalate (bulk salvation), (b) adipate (bulk salvation), (c) suberate (surface salvation), and (d) tetradecandioic dianion (surface salvation).

hydrophilic and hydrophobic forces is seen in density profiles shown in Figure 5b. Clearly, for this dianion the former forces won over the latter resulting in the interior solvation of adipate.

4.3. Suberate: $^{-}O_2C(CH_2)_6CO_2^{-}$. The aqueous clusters of suberate were the topic of our previous joint experimental and theoretical investigation.[32] In particular, experimentally inferred folding was born out nicely from the MD simulations. These cluster studies suggested that suberate would exhibit an interesting behavior in the interface with its hydrophobic aliphatic chain point out of the solution. This is clearly born out in the current MD simulation of an extended slab, as shown in the density profiles of aqueous suberate (Figure 5c). We see that upon moving from a dicarboxylate dianion with four to six CH_2 groups a transition from bulk to surface solvation occurred. This is demonstrated in Figure 5c by the signal from the aliphatic carbons, which peaks right at the water/vapor interface. Note that the signal of the carboxylate oxygens peaks closer to the bulk aqueous region than that of the carbon atoms. This reflects a generic pattern of longer, surface-solvated dicarboxylate dianions with the hydrophilic $-CO_2^{-}$ groups immersed in the surface solvent layer and the hydrophobic aliphatic chain repelled from water and, consequently, somewhat bent, analogous to the picture derived from our previous cluster study. Figure 6 shows a typical snapshot from the MD simulation, displaying the aqueous surface with the suberate dianion and demonstrating clearly this surface solvation behavior. Finally, note that the counterions also reside at the same side of the slab as suberate, albeit much deeper in the aqueous phase. Sodium cations themselves have no propensity for the water/vapor interface, but rather they tend to neutralize the charges of the dicarboxylate dianion.

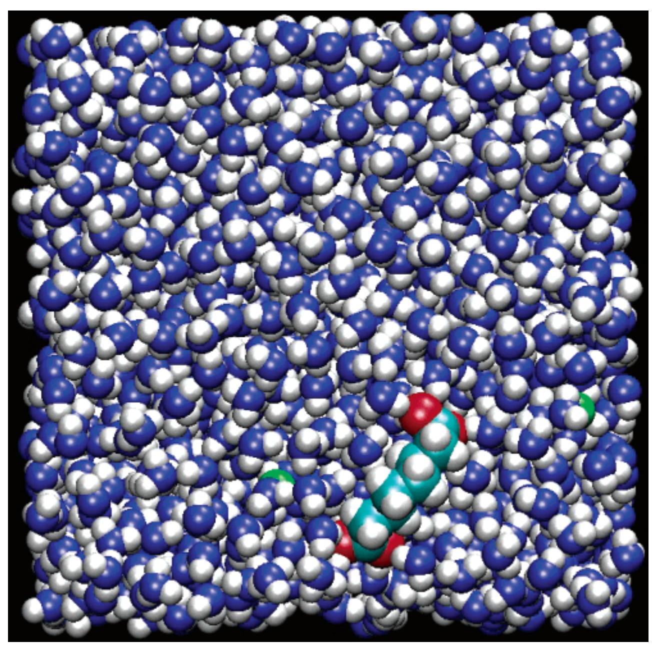

Figure 6. Typical snapshot from the simulation showing the surface-solvated suberate ion with the carboxylate groups solvated in the interfacial layer and the aliphatic carbon chain sticking into the vapor phase.

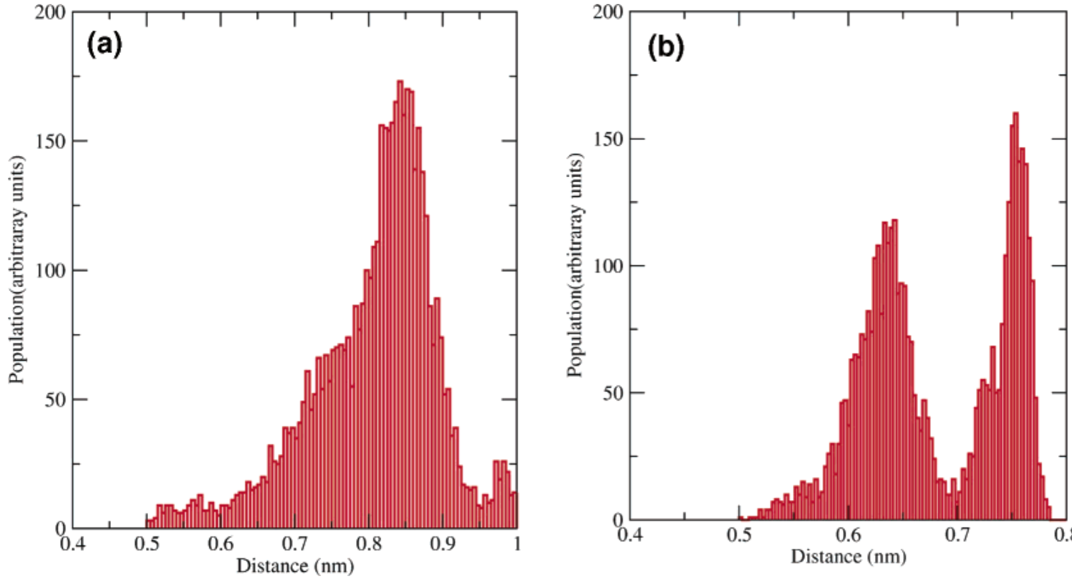

Figure 7. Distributions of carboxylate carbon−carbon distances for aqueous (a) adipate and (b) suberate. Unfolded structures dominate the bulk-solvated adipate, while suberate folds at the water/vapor interface.

4.4. The Tetradecandioic Dianion: $^{-}O_2C(CH_2)_{12}CO_2^{-}$. Upon prolonging the aliphatic chain of the dicarboxylate dianion the hydrophobic interactions can only become stronger and the aqueous surface solvation pertains. Figure 5d shows the density profiles for the largest investigated system, the tetradecandioic dianion. We see that the propensity of the dianion for the water/vapor interface is even stronger than in the case of suberate. Again, the aliphatic chain bends and sticks out into the vapor phase, while the carboxylate groups tend to solvate in the interfacial layer of the aqueous phase. The tendency of the sodium counterions to follow the dianion also pertains.

4.5. Folding of the Aliphatic Chains in the Water/Vapor Interface. A typical feature present in all but the shortest dicarboxylate dianions is the possible existence of a collinear and various folded structures due to the flexibility of the aliphatic chain. While in the gas phase all the dicarboxylate dianions tend to be collinear because of a strong Coulombic repulsion between the two carboxylate groups,[34] in an aqueous environment an efficient dielectric screening of the charged groups allows also for the occurrence of folded geometries. It is illuminating to compare the distribution in the aqueous slab of structures of a short, bulk-solvated adipate (see Figure 7a) with that of the longer, surface-solvated suberate (Figure 7b). In the case of adipate collinear geometries, corresponding to a distance between the carboxylate groups of 8−9 Å dominate. The situation is to some extent reversed for the surface-solvated suberate (Figure 7b). Because of the hydrophobic interactions of the aliphatic chain, which is pushed out of the aqueous phase, the suberate dianion tends to bend to solvate at the same time as the charged carboxylate groups. This corresponds to the peaks at 6.5 Å and 7.5 Å in Figure 7b, which reflect different degrees of folding of the aliphatic chain.

4.6. Solvation Structures of the Carboxylates. There is another interesting question pertaining to the bulk vs interfacial solvation of dicarboxylate dianions of varying aliphatic chain length. What is the structure of water molecules around the hydrophilic carboxylate groups, and are there differences between bulk- and surface-solvated dianions? A typical geometry of adipate with the surrounding 30 water molecules is depicted in Figure 8a, while a similar snapshot from a MD simulation of aqueous suberate is shown in Figure 8b. In both cases, the charged carboxylate groups are strongly hydrated. While the short aliphatic chain of the bulk-solvated adipate "squeezes" within the aqueous solvation shell, that of suberate is too long and is pushed out from the aqueous phase.

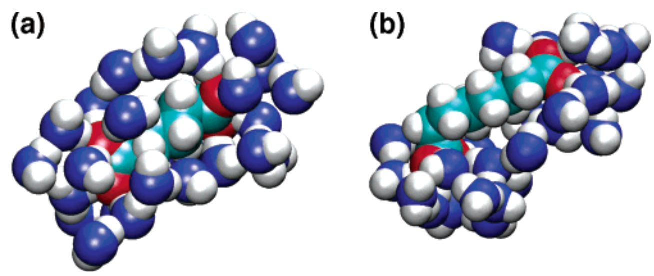

Figure 8. Structure of the solvation shell around (a) adipate and (b) suberate. While in the former case water molecules encompass the whole dianion, in the latter case the aliphatic chain remains unsolvated.

We have quantified the solvation structures in terms of radial distribution functions. Figure 9 shows the carboxylate oxygen−water oxygen radial distribution functions for adipate and suberate. On the first view the two curves look similar, with the first sharp (second broad and, in the case of suberate, somewhat structured) maximum corresponding to the first (second) solvation shell, despite the fact that the adipate solvates in the aqueous bulk while suberate sovates at the water/vapor interface. However, the integrals under the first peak, which give the numbers of the water molecules in the first solvation shell, are different for the two cases. Namely, while there are roughly seven water molecules around each of the carboxylate groups of the bulk-solvated adipate, this number drops to five for the surface-solvated suberate. We note that the first solvation shell of five waters in the surface-solvated suberate agrees remarkably well with the solvated cluster results. These show a negligible even−odd effect in the measured ADEs once each carboxylate is solvated by five waters since additional waters do not interact with the negative charges directly, i.e., they are added to the second solvation shell. Note that the first solvation shell derived from the solvated clusters of the tetradecandioic

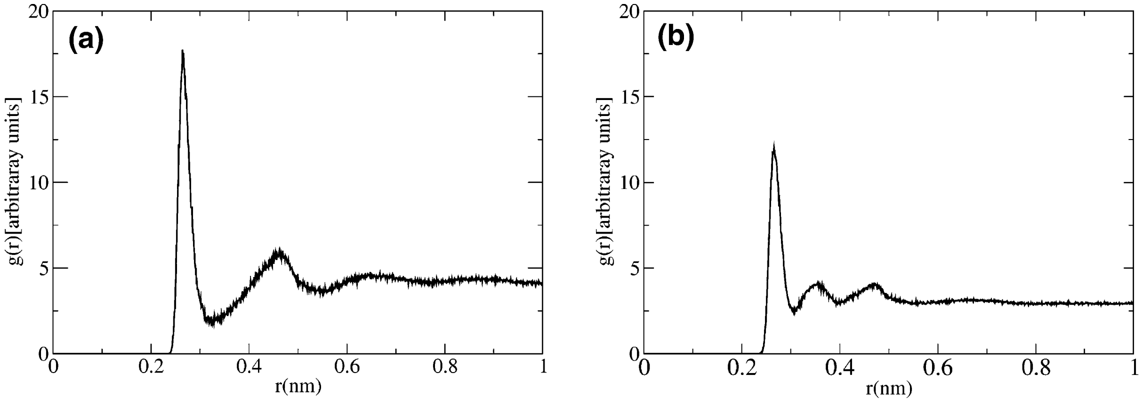

Figure 9. Carboxylate oxygen−water oxygen radial distribution functions for (a) adipate and (b) suberate.

dianion, which is surface-solvated as well, contains also five waters for each carboxylate group, as discussed above (see Section 3.3.3.).

5. Conclusions

We have investigated using molecular dynamics simulations and photoelectron spectroscopy aqueous solvation of a series of dicarboxylate dianions with 0, 2, 4, 6, and 12 CH_2 groups of the aliphatic chain connecting the two carboxylate groups. Photoelectron spectra of solvated clusters of succinate, adipate, and tetradecandioic dianions with up to 20 water molecules were obtained. Together with previous reports on solvated oxalate and suberate,[30−32] a relatively complete data set for solvated dicarboxylates with various chain lengths is available now. The isolated succinate dianion was observed for the first time and was shown to have an adiabatic electronic binding energy of ~0.0 eV, being the smallest stable dicarboxylate dianion. Photoelectron data of solvated succinate were consistent with an interior solvation state for this dianion. The electron binding energies as a function of solvation revealed for adipate that there was a small conformational change between 12 and 13 solvent molecules. The most pronounced even−odd effect was observed for the electron binding energies of the tetradecandioic dianion. The effect tapered off above 10 water molecules, suggesting that the first five water molecules form the first solvation shell for each of the carboxylate groups. A folding conformation change is expected for the tetradecandioic dianion as a function of solvation because of the hydrophobic interactions between water and the aliphatic chain and the strong water−water interactions; however, it was not observed within the currently accessible size range of up to 18 water molecules. This folding is likely to take place at larger sizes because of the entropic stabilization of the linear conformation at finite temperatures.

Molecular dynamics simulations revealed that the smallest of dicarboxylate dianions, oxalate, solvates deep in the aqueous bulk, similarly to other small dianions containing no hydrophobic group, such as sulfate. For all short dicarboxylate dianions up to adipate bulk aqueous solvation prevails, since hydrophilic interactions of the charged carboxylate groups win over the hydrophobic forces due to the aliphatic chain. However, upon further increasing the aliphatic chain length hydrophobic interactions overwhelm the hydrophilic ones. As a result, suberate and longer dicarboxylate dianion have a strong propensity for the water/vapor interface. This change of the aqueous solvation behavior of dicarboxylate dianions upon increasing the lengths of the aliphatic chain is in accord with the solubility data of the corresponding acids (obtainable, e.g., from the Beilstein database). Namely, the transition between soluble and insoluble acids correlates with that between the bulk vs surface located dianions, while oxalic, malonic, succinic, and glutaric acids are strongly soluble in water and adipic acid is moderately soluble, subaric acid is only slightly soluble, and acids with longer aliphatic chains are practically insoluble in water.

The bulk vs surface solvation of dicarboxylate dianions also has an effect on the structure of aqueous solvation shells and on the folding of the flexible aliphatic chain. Small bulk-solvated dicarboxylate dianions prefer more unfolded structures and a larger number of water molecules in the solvation shells around the carboxylate groups than large surface-solvated dianions.

Acknowledgment. The experimental work was supported by the U.S. Department of Energy (DOE), Office of Basic Energy Sciences, Chemical Science Division, and performed at EMSL, a national scientific user facility sponsored by DOE's Office of Biological and Environmental Research and located at Pacific Northwest National Laboratory, operated for DOE by Battelle. Support (to P.J.) from the Czech Ministry of Education (Grant LN00A032) and the National Science Foundation (Grant CHE-0209719) is gratefully acknowledged. Part of the work in Prague was completed within the framework of research project Z4 055 905.

JA047493I